Nanoparticles

Core/Shell Gold Nanoparticles by Self-Assembly and Crosslinking of Micellar, Block-Copolymer Shells**

*Youngjong Kang and T. Andrew Taton**

Core/shell nanoparticle architectures, in which a layer of inorganic or organic material surrounds an inorganic nanoparticle core, have been investigated both as a means to improve the stability and surface chemistry of the core nanoparticle and as a way of accessing unique physical properties that are not possible from one nanomaterial alone. As examples, silica shells isolate metal and semiconductor particle surfaces from interfacial chemistry;[1,2] gold shells allow covalent attachment of thiol ligands to particles[3] and generate unique optical signatures;[4] semiconductor shells increase the quantum yield of semiconductor nanoparticle cores;[5] and polymeric shells aid the compatibility of nanoparticles in polymer hosts.[6] Whereas inorganic shells are typically grown from the surface of the particle core, a number of methods have been described for generating organic polymer shells, including polymerization from particle-bound initiators,[7] direct attachment of functionalized polymers to surfaces,[8] layer-by-layer deposition,[9] and synthesis of the particle in the presence of polymeric ligand.[10,11] In all of these cases, the specific chemical interaction of the particle surface and the surface-bound polymer must be explicitly tailored in order to form the shell.

Diblock copolymer amphiphiles spontaneously form polymer monolayers on surfaces, and the thickness and composition of the assembled layer are determined by the lengths and properties of the component blocks.[12] Because this assembly can be driven by desolvation of one of the two polymer blocks and does not depend on any specific polymer–surface interaction, we hypothesized that block copolymers could be used to form shells around nanoparticle cores without chemical anchoring. Herein, we report the assembly of metal-core, block-copolymer-shell nanoparticles in which the structure and composition of the combined material are programmed in advance by the choice of particle and copolymer starting materials. Furthermore, we demonstrate that cross-linking the assembled shell leads to a permanent core/shell structure and physically isolates the core from its environment.

[*] Y. Kang, Prof. T. A. Taton
Department of Chemistry
University of Minnesota
207 Pleasant St SE, Minneapolis, MN 55455 (USA)
Fax: (+1) 612-626-7541
E-mail: taton@chem.umn.edu

[**] We thank the ACS Petroleum Research Fund for partial support of this research.

Supporting information for this article is available on the WWW under http://www.angewandte.org or from the author.

 DOI: 10.1002/ange.200461119

Our approach to the synthesis of copolymer-encapsulated nanoparticles (Scheme 1) employs block copolymers and cross-linking chemistry that were developed by Wooley and co-workers for shell-crosslinked micelles.[13] Briefly, poly(styrene-block-acrylic acid) (PS-b-PAA) and poly(methylmethacrylate-block-acrylic acid) (PMMA-b-PAA) copolymer surfactants with narrow molecular-weight polydispersities (PDI < 1.3) were synthesized through atom-transfer radical polymerization.[14,15] Amphiphilic copolymer was initially dissolved in DMF (*N*,*N*-dimethylformamide), which is a good solvent for both the hydrophobic (PS or PMMA) and the hydrophilic (PAA) polymer blocks. Citrate-capped Au nanoparticles[15,16] in aqueous solution were centrifuged and resuspended in DMF. The samples of polymer and nanoparticles in DMF were combined in the presence of a small amount of 1-dodecanethiol, which hydrophobically functionalizes the surfaces of the particles and directs them to the hydrophobic interior of a micellar shell.[17] Water was gradually added to this mixture to simultaneously desolvate both the particles and the hydrophobic polymer block from solution. In the absence of copolymer surfactant, the dodecanethiol-modified nanoparticles precipitated quickly from DMF as water was added. In the absence of dodecanethiol, the nanoparticles remained outside the assembled block-copolymer micelles. Transmission electron microscopy (TEM) images of these assemblies indicated that the external polyacrylate block of the micelles associated with the surfaces of the nanoparticles (Figure 1 a)[18] presumably by displacing bound citrate. However, for dodecanethiol-functionalized Au, the added water acted as a selective nonsolvent (that is, a solvent that does not solubilize a specific material) for both the hydrophobic polymer block and the hydrophobically modified nanoparticles and induced the formation of micelles around the nanoparticles (Figure 1 b). Micelle encapsulation was conducted with a substantial excess of polymer to limit the number of micelles that contained multiple particles. This process was successful for polymers with short PAA blocks (PS_{250}-b-PAA_{13}, PS_{160}-b-PAA_{13}, PS_{100}-b-PAA_{13}, and $PMMA_{240}$-b-PAA_{13}).[15]

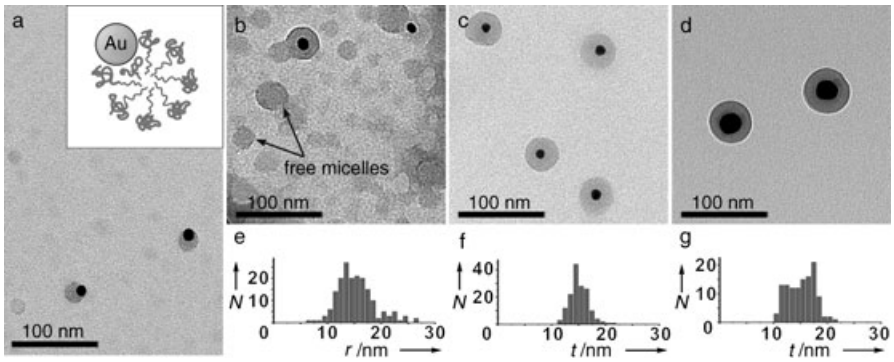

Figure 1. a–d) TEM images of Au nanoparticles encapsulated within PS_{250}-b-PAA_{13} micelles. a) Poorly encapsulated 12-nm Au nanoparticles exposed to PS_{250}-b-PAA_{13} in the absence of dodecanethiol. Empty copolymer micelles distort to maximize interactions between the polyacrylate corona and the surface of the Au nanoparticle. b) Encapsulated Au nanoparticles treated with dodecanethiol and PS_{250}-b-PAA_{13}, before purification. Nanoparticles are localized at the center of the micelles. c) Purified encapsulated 12-nm Au nanoparticles. d) Purified encapsulated 31-nm Au nanoparticles. e–g) Histograms of e) the radius (r) of empty micelles isolated from encapsulated 12-nm Au nanoparticle supernatant, f) the shell thickness (*t*) of encapsulated 12-nm Au nanoparticles, and g) the shell thickness of encapsulated 31-nm Au nanoparticles. *N* = number. See Supporting Information for the TEM images used to obtain the histograms.

The assembled copolymer was permanently fixed by cross-linking the polyacrylate block of the micelles with 2,2′-(ethylenedioxy)bis(ethylamine) and 1-(3-dimethylaminopropyl)-3-ethylcarbodiimide methiodide in water (see Scheme 1). After cross-linking, excess reagents were removed by dialysis of the suspension against H_2O. Fixed core/shell nanoparticles were separated from empty micelles by five or more consecutive cycles whereby the suspension was centrifuged, the supernatant was discarded, and the solid was resuspended in H_2O. After this treatment, the suspension consisted solely of micelles filled with Au nanoparticles (Figure 1, c and d). For Au nanoparticles larger than 10 nm in diameter, every micelle contained exactly one nanoparticle. Despite our presumption that a statistical distribution of particles might lead to a few micelles that contain two or more particles, no such structures were observed. For smaller (4-nm diameter) nanoparticles, however, multiple particles were sometimes encapsulated in each micelle.[15] Averaged over

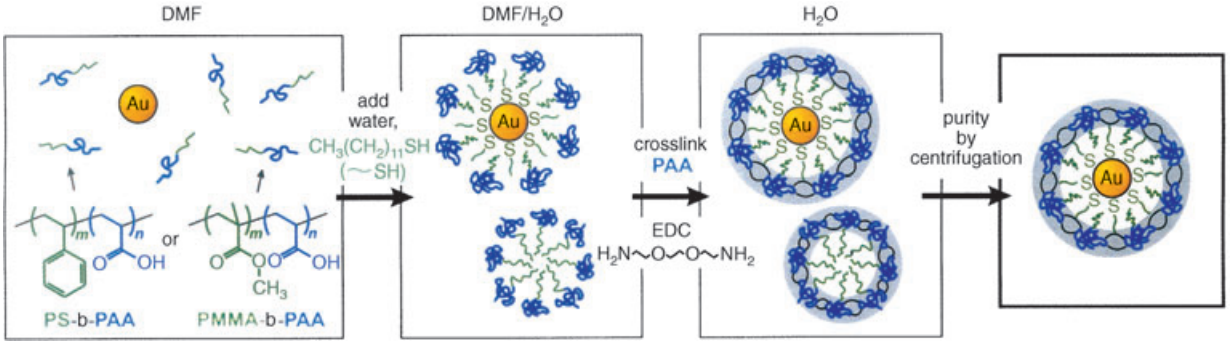

Scheme 1. Preparation of core/shell gold nanoparticles. EDC = *N*-ethyl-*N*′-(3-dimethylaminopropyl)carbodiimide.

more than 100 particles, the shell thicknesses for 12- and 31-nm Au nanoparticles encapsulated in PS_{250}-b-PAA_{13} ("Au@PS_{250}-b-PAA_{13}") were 15.1 ± 1.7 nm and 15.2 ± 2.5 nm, respectively, whereas the average radius of empty PS_{250}-b-PAA_{13} micelles isolated from the encapsulated 12-nm Au nanoparticle solution was 15.2 ± 3.5 nm. So, whereas the copolymer shell thickness could be predicted on the basis of the radius of empty copolymer micelles, the shells were consistently more uniform in size than the micelles. The fact that only single nanoparticles were found in each micelle as well as the uniformity of the micellar shells suggest that the encapsulated particles offer a spherical surface template for micelle assembly. Flat surfaces have been shown to template the formation of uniform surface layers of block copolymers.[12] Here we demonstrate that this phenomenon is observed even when the curvature of the surface is smaller in scale than the thickness of the polymer layer. This is surprising given that the micelles are much larger than the nanoparticles and could presumably accommodate multiple particle guests.

The optical properties of the Au nanoparticles can be controlled by variation of the composition of the copolymer shell which is consistent with the theoretical prediction that surface plasmon resonance energies decrease as the refractive index of the surrounding medium increases.[19] In water ($n = 1.33$), citrate-capped 31-nm-diameter Au particles show a characteristic absorbance maximum $\lambda_{max} = 529$ nm (Figure 2a). However, the higher refractive indices of PMMA

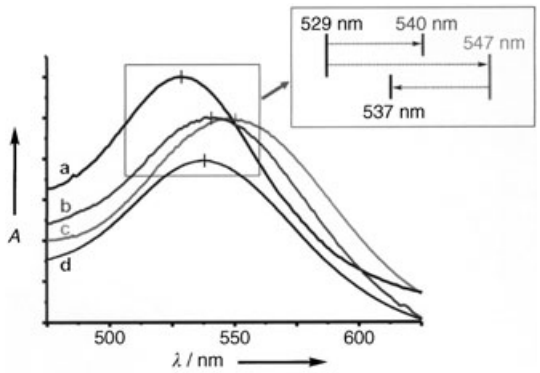

Figure 2. Shift of the surface plasmon resonance spectra upon encapsulation of Au nanoparticles (absorbance intensities are normalized). a) The absorbance spectrum of aqueous 31-nm-diameter gold nanoparticles. The spectrum is red-shifted by encapsulation within $PMMA_{240}$-b-PAA_{13} (b) or within PS_{250}-b-PAA_{13} (c). The spectrum is blue-shifted when the PS_{250}-b-PAA_{13} polymer shell is swollen with THF (d).

($n = 1.49$) and PS ($n = 1.59$) lead to red-shifted absorbance spectra for Au@$PMMA_{240}$-b-PAA_{13} ($\lambda_{max} = 540$ nm) and Au@PS_{250}-b-PAA_{13} ($\lambda_{max} = 547$ nm; see Figure 2, b and c). Similar plasmon shifts have been reported for Au nanoparticles within silica shells[1,20] in which the higher refractive index of SiO_2 ($n = 1.47$) results in higher values of λ_{max}.

In water, the glassy polystyrene block of the cross-linked copolymer shells provides a physical barrier that isolates and protects encapsulated nanoparticles from their chemical environment. When exposed to aqueous cyanide etching solution, citrate-capped gold nanoparticles are typically oxidized to $[Au(CN)_2]^-$ ions within seconds. Copolymer-encapsulated Au nanoparticles were stable indefinitely to much higher concentrations of etchant (Figure 3). By con-

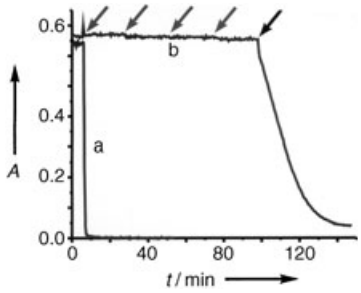

Figure 3. a) Cyanide-induced decomposition of citrate-stabilized, 12-nm Au nanoparticles in water. Similar, immediate decomposition was observed for dodecanethiol-stabilized nanoparticles.[15] b) Exposure of encapsulated 12-nm Au nanoparticles (within a PS_{250}-b-PAA_{13} shell) in water to a 25-fold molar excess of KCN (5-mM aqueous solution) every 20 min (gray arrows; total 100-fold molar excess), followed by the addition of 20 vol% THF after 100 min (black arrow). The absorbance was measured at the values of λ_{max} (519 nm and 529 nm for curves a and b, respectively). The initial 8% drop of absorbance upon addition of THF is attributed to a change in the refractive index of the solvent.[15]

trast, surface-bound molecular[21] and homopolymer[11] monolayers and silica shells[22] have been shown to be permeable with respect to cyanide corrosion. The permeability of the micellar shell could be modulated by addition of an organic cosolvent to the aqueous suspension of the particles to solvate the hydrophobic polymer block. For example, addition of 20 vol% THF to the suspension of encapsulated Au nanoparticles in a solution containing cyanide resulted in immediate etching (Figure 3). Variation of the degree of shell cross-linking had no effect on the extent or rate of etching which demonstrates that solvation of the shell, rather than the physical porosity of the polymer network, regulates exposure to etching. Further evidence of THF infiltration and swelling of the inner micelle block with THF was observed by a blue shift of the optical absorbance spectrum of the nanoparticles (in the absence of cyanide, Figure 2d). This shift reflects the contribution of the lower refractive index of THF ($n = 1.41$) to the PS environment around each nanoparticle.

Even though organic solvents solubilize the hydrophobic micelle block, chemical cross-links prevent the surfactant from dissolving away. As a result, micelle-encapsulated nanoparticles were found to be soluble in essentially any solvent that was compatible with either the hydrophobic or hydrophilic component polymers.[15] For example, nanoparticles encapsulated in PS-b-PAA were soluble in solvents in which PS can be dissolved, but notably not in acetone or 1:1 *i*PrOH/MEK (methyl ethyl ketone), which are both nonsolvents for PS. Also, nanoparticles encapsulated in PMMA-b-PAA were soluble in solvents in which PMMA can be dissolved, but not in cyclohexane, which is a nonsolvent for PMMA.

Because the shells were fixed, the solvated polymer cores could be desolvated again to regenerate the original glassy core/shell nanostructures. Au@PS_{250}-b-PAA_{13} particles dis-

solved in an organic solvent such as THF could be returned to aqueous solution by exhaustive dialysis against H_2O. TEM images of these particles were indistinguishable from images of the originally synthesized, aqueous particles. On the basis of these results, we anticipate that copolymer micelle encapsulation could be used as a general aid to disperse nanoparticles in otherwise incompatible matrices. Along these lines, Au@PS_{250}-b-PAA_{13} was readily dispersed from solvent into bulk PS, and Au@$PMMA_{240}$-b-PAA_{13} into bulk PMMA, to form homogeneously pink-colored composite plastics.

In conclusion, we have demonstrated surface-templated self-assembly of copolymers around nanoparticles as a route to defined core/shell nanostructures. This approach yielded core/shell architectures in which the dimensions and properties of the nanostructures were determined by the characteristics of the component polymer blocks. We are currently applying this approach to other lyophilic nanoparticles such as TOPO-coated quantum dots[23] and oleic acid coated magnetic nanoparticles.[24] We anticipate that micelle encapsulation will allow shell functionalization, biomolecular conjugation, and polymer processing to be performed on nanomaterials that might otherwise show poor or no ligand chemistry.[25]

Received: June 29, 2004
Revised: August 26, 2004

Keywords: block copolymers · layered compounds · micelles · nanostructures · self-assembly

[1] L. M. Liz-Marzan, M. Giersig, P. Mulvaney, *Langmuir* **1996**, *12*, 4329 – 4335.
[2] a) K. Kamata, Y. Lu, Y. N. Xia, *J. Am. Chem. Soc.* **2003**, *125*, 2384 – 2385; b) D. Gerion, F. Pinaud, S. C. Williams, W. J. Parak, D. Zanchet, S. Weiss, A. P. Alivisatos, *J. Phys. Chem. B* **2001**, *105*, 8861 – 8871; c) S. P. Mulvaney, M. D. Musick, C. D. Keating, M. J. Natan, *Langmuir* **2003**, *19*, 4784 – 4790.
[3] a) Y. Cao, R. Jin, C. A. Mirkin, *J. Am. Chem. Soc.* **2001**, *123*, 7961 – 7962; b) J. L. Lyon, D. A. Fleming, M. B. Stone, P. Schiffer, M. E. Williams, *Nano Lett.* **2004**, *4*, 719 – 723.
[4] R. D. Averitt, D. Sarkar, N. J. Halas, *Phys. Rev. Lett.* **1997**, *78*, 4217 – 4220.
[5] M. A. Hines, P. Guyot-Sionnest, *J. Phys. Chem.* **1996**, *100*, 468 – 471.
[6] a) M. K. Corbierre, N. S. Cameron, M. Sutton, S. G. J. Mochrie, L. B. Lurio, A. Ruehm, R. B. Lennox, *J. Am. Chem. Soc.* **2001**, *123*, 10411 – 10412; b) S. Kim, M. G. Bawendi, *J. Am. Chem. Soc.* **2003**, *125*, 14652 – 14653.
[7] a) C. R. Vestal, Z. J. Zhang, *J. Am. Chem. Soc.* **2002**, *124*, 14312 – 14313; b) S. Nuss, H. Bottcher, H. Wurm, M. L. Hallensleben, *Angew. Chem.* **2001**, *113*, 4137 – 4139; *Angew. Chem. Int. Ed.* **2001**, *40*, 4016 – 4018; c) T. von Werne, T. E. Patten, *J. Am. Chem. Soc.* **2001**, *123*, 7497 – 7505; d) K. Sill, T. Emrick, *Chem. Mater.* **2004**, *16*, 1240 – 1243.
[8] a) M.-Q. Zhu, L.-Q. Wang, G. J. Exarhos, A. D. Q. Li, *J. Am. Chem. Soc.* **2004**, *126*, 2656 – 2657; b) M. K. Corbierre, N. S. Cameron, R. B. Lennox, *Langmuir* **2004**, *20*, 2867 – 2873.
[9] D. I. Gittins, F. Caruso, *J. Phys. Chem. B* **2001**, *105*, 6846 – 6852.
[10] a) A. B. Lowe, B. S. Sumerlin, M. S. Donovan, C. L. McCormick, *J. Am. Chem. Soc.* **2002**, *124*, 11562 – 11563; b) K. J. Watson, J. Zhu, S. T. Nguyen, C. A. Mirkin, *J. Am. Chem. Soc.* **1999**, *121*, 462 – 463.
[11] W. P. Wuelfing, S. M. Gross, D. T. Miles, R. W. Murray, *J. Am. Chem. Soc.* **1998**, *120*, 12696 – 12697.
[12] A. Halperin, M. Tirrell, T. P. Lodge, *Adv. Polym. Sci.* **1992**, *100*, 31 – 71.
[13] H. Y. Huang, T. Kowalewski, E. E. Remsen, R. Gertzmann, K. L. Wooley, *J. Am. Chem. Soc.* **1997**, *119*, 11653 – 11659.
[14] K. Matyjaszewski, J. Xia, *Chem. Rev.* **2001**, *101*, 2921 – 2990.
[15] See Supporting Information for further details of synthesis and characterization.
[16] a) G. Frens, *J. Nat. Phys. Sci.* **1973**, *241*, 20 – 22; b) K. R. Brown, D. G. Walter, M. J. Natan, *Chem. Mater.* **2000**, *12*, 306 – 313.
[17] A prerequisite of our encapsulation method is that the starting nanoparticles must be transiently stable in the encapsulation medium. Large (diameter > 5 nm), citrate-capped nanoparticles slowly precipitate from suspension in the presence of alkanethiol ligands, so the nanoparticles were functionalized with alkanethiol in situ. However, smaller alkanethiol-functionalized particles were prepared separately before encapsulation.
[18] I. Hussain, M. Brust, A. J. Papworth, A. I. Cooper, *Langmuir* **2003**, *19*, 4831 – 4835.
[19] a) T. R. Jensen, M. L. Duval, K. L. Kelly, A. A. Lazarides, G. C. Schatz, R. P. Van Duyne, *J. Phys. Chem. B* **1999**, *103*, 9846 – 9853; b) A. C. Templeton, J. J. Pietron, R. W. Murray, P. Mulvaney, *J. Phys. Chem. B* **2000**, *104*, 564 – 570.
[20] Y. Lu, Y. D. Yin, Z. Y. Li, Y. A. Xia, *Nano Lett.* **2002**, *2*, 785 – 788.
[21] a) T. Zhu, K. Vasilev, M. Kreiter, S. Mittler, W. Knoll, *Langmuir* **2003**, *19*, 9518 – 9525; b) R. Paulini, B. L. Frankamp, V. M. Rotello, *Langmuir* **2002**, *18*, 2368 – 2373.
[22] T. Ung, L. M. Liz-Marzan, P. Mulvaney, *Langmuir* **1998**, *14*, 3740 – 3748.
[23] D. V. Talapin, A. L. Rogach, A. Kornowski, M. Haase, H. Weller, *Nano Lett.* **2001**, *1*, 207 – 211.
[24] T. Hyeon, S. S. Lee, J. Park, Y. Chung, H. Bin Na, *J. Am. Chem. Soc.* **2001**, *123*, 12798 – 12801.
[25] Y. J. Kang, T. A. Taton, *J. Am. Chem. Soc.* **2003**, *125*, 5650 – 5651.

